ELSEVIER

Thermochimica Acta 295 (1997) 147–165

thermochimica acta

Thermostimulated inert gas release analysis in the diagnostics of materials[1]

V. Balek[a,*], I.N. Beckman[b]

[a] *Nuclear Research Institute, CZ–25068 Rez, Czech Republic*
[b] *Chemical Faculty, Moscow State University, Moscow 199234, Russian Federation*

Abstract

The principles of thermostimulated inert gas release analysis (TIGRA), based on the measurements of inert gas migration in solids, are given. Methodological bases and the computer treatment of the TIGRA results are described. The potential and various applications of this method are demonstrated, e.g. the determination of inert gas mobility in metals, polymers, ionic crystals and ceramics, the characterization of non- crystalline solids and their changes. © 1997 Elsevier Science B.V.

Keywords: Thermostimulated; Gas release analysis; Diagnostic

1. Introduction

The Evolved Gas Analysis (EGA) is known as an appropriate method for characterisation of reactions in solids accompanied by gas evolution.

During the past two decades, the family of EGA techniques has been increased by TIGRA. The TIGRA is based on the measurement of inert gases released from solids, usually previously labelled by the inert gas [1]. The atoms of inert gases (from helium to radon) are used as trace indicators or a microprobe of the defect state of the solid and its changes. Radioactive nuclides of inert gases (e.g. ^{24}Ne, ^{39}Kr, ^{133}Xe, 222Rn), can be advantageously used as the probe of solids due to their easy detection in trace concentrations. Noble gases of "smaller size" such as He, Ne (the atomic radius of Ne is 0.112 nm) can be applied in the study of the single point defects, whereas the "large sized" noble gases, such as Kr, Xe, Rn (the atomic radius of Rn is 0.214 nm) can be used in the complex defects mobility assessment, in the investigation of the morphology formations of solids and their changes. The inert gas atoms do not react with the solid matrix and their release is controlled primarily by diffusion. The processes which influence the inert gas diffusion in the solid matrix and pores, or surface area of the sample, can be revealed by this method. Minor effects in the solid unaccompanied by changes in sample mass or enthalpy, which cannot be investigated by thermogravimetry or DTA, respectively, can be investigated by TIGRA. This method makes it possible to gain information about the defects and irregularities of the structure of solids, which is complementary to the information given by other methods, i.e. X-ray diffraction. The TIGRA can be used in the study of both crystalline and non-crystalline materials [2,3].

In this paper methodical bases for the application of the TIGRA to the diagnostics of materials are given.

2. Labelling of solid samples by the noble gases

In general, common inert (noble) gases and their radioactive isotopes or natural radioactive inert gases

*Corresponding author.

[1] The paper is dedicated to Dr. H.J. Matzke on the occasion of his 60th birthday.

PII S0040-6031(97)00104-4

(such as radon) can be used for the TIGRA-measurements.

Most of the solids to be investigated by TIGRA naturally do not contain inert gas and it is necessary to label them with a trace amount of the inert gas. The conditions of high energy gas ions, high temperature and high gas pressure are required for impelling the inert gas into solids.

There are a number of techniques which can be used for direct incorporation of inert gas atoms in solids. All of them are characterized by a definite quantity of the introduced gas which decreases during storage or measurement. The choice of the technique for inert gas introduction depends mainly on the character of the solid to be labelled and the aim for which the labelled solid should be prepared.

2.1. Diffusion technique

This is based on the diffusion of the inert gas into solids at elevated temperatures and pressure of the gas. The substance to be labelled and the inert gas are placed in a high-pressure vessel which is then closed and heated for several hours at the temperature of approximately 0.3–0.5 T_{melt} of the substance to be labelled, and finally quenched in liquid nitrogen. The amount of inert gas introduced into the sample depends on time, temperature and pressure, as given by the diffusion equation [1].

The diffusion technique was used to introduce ^{85}Kr in more than 250 different solids including metals, inorganic and organic compounds in the form of foils, powders and single crystals. A microdiffusion technique for labelling powders permitting the reduction of the losses of residual inert gas was proposed [4,5].

2.2. Physical vapour deposition

In this method, thin films produced in an inert gas atmosphere (e.g. argon) are automatically labelled by the inert gas. The inert gas atoms are captured in the structure of the deposited substance. The release of the gas can be used for diagnostics of the film during its subsequent heating.

2.3. Implantation of accelerated ions of inert gases

The amount of inert gas introduced and its concentration profile depends on the energy of ion bombardment and the properties of the labelled matrix. A number of techniques can be used for inert gas ion bombardment [6–8]. A defined ion beam can be produced using a magnetic separator. A versatile low-cost technique for sample labelling was invented by Jech [9].

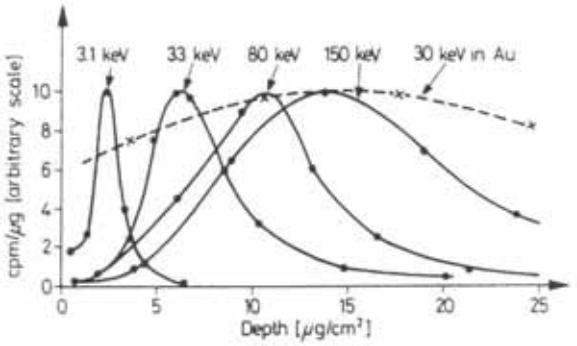

Fig. 1. Differential range distribution curves normalised to the peak height for ^{133}Xe in Al and Au targets. The bombarded energy is indicated beside each curve (●–Al ×–Au).

Fig. 1 gives curves of the differential distribution of xenon atoms in aluminium and gold [8]. Energies from 3.1–150 keV were employed. The distribution profiles distinctly indicate non-uniform distribution. The distribution of the embedded atoms is seen to consist of an asymmetric peak with an exponential tail. With an increase in the energy of the ions the maximum is shifted towards greater distances from the surface. In addition, the range distribution curves are much narrower for materials consisting of light elements (with lower Z) such as aluminium, than for heavier elements, such as gold. The distribution curves are considerably broadened when a large integral flux is used ($>10^{10}$ ions/cm^2) during a long bombardment, peaking at a lower penetration depth. The peak occurs at only half the depth observed in the trace bombardment. The deep penetrations are typical channelling events and are markedly different from the isotropic (amorphous) solid. Direction ⟨110⟩ exhibits the deepest penetration.

2.4. Inert gases produced from nuclear reactions

The recoil energy of nuclear reactions producing inert gases can be used for the implantation of gases into solid samples, e.g. in alkali-metal or alkaline earth metal halides Ar, Kr, and Xe are formed by means of (n, α) and (n, p) reaction, respectively. Nuclear fission reactions have been used for the incorporation of the

Table 1
Nuclear reactions which can be used for production of inert gas atoms and their introduction into solid samples

α-decay	$^{226}Ra \rightarrow^{\alpha} 222Rn$ $^{228}Th \rightarrow^{\alpha} 224Ra \rightarrow^{\alpha} 220Rn$
β-decay	$^{83}Se \rightarrow^{-\beta} 83Br \rightarrow^{-\beta} 83Kr$ $^{133}Te \rightarrow^{-\beta} 133I \rightarrow^{-\beta} 133Xe$
(n, α)	$^{40}Ca(n, \alpha)\ ^{137}Ar$ $^{88}Sr(n, \alpha)\ ^{85m}Kr$ $^{136}Ba\ (n, \alpha)\ ^{133}Xe$
(n, p)	$^{39}K(n, p)\ ^{39}Ar$ $^{85}Rb(n, p)\ ^{85}Kr$ $^{133}Cs\ (n, p)\ ^{133m}Xe$
(n, γ) and β-decay	$^{37}Cl(n, \gamma)^{38}Cl \rightarrow^{-\beta} 38Ar$ $^{79}Br(n, \lambda)^{80}Br \rightarrow^{-\beta} 80Kr$ $^{127}I(n, \gamma)^{128}I \rightarrow^{-\beta} 128Xe$
Fission (n, f)	$^{238}U(n, f)Xe, Kr, \ldots$

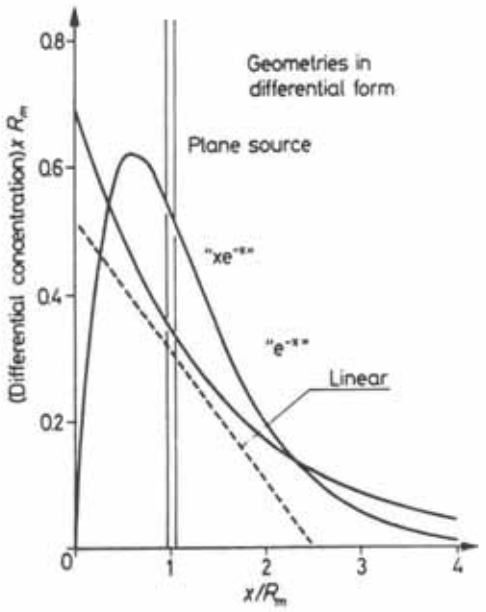

Fig. 2. Idealized concentration profiles suited for ion bombardment, recoil and diffusion techniques of labelling.

radionuclides of ^{133}Xe and ^{85}Kr. Some of the nuclear reactions which have been used for the production of inert gas atoms and their introduction into solid samples are listed in Table 1 in [1].

By varying the conditions for labelling (e.g. neutron flux, type of the nuclear reaction, dose and energy in ion bombardment), it is possible to separate different release processes which could otherwise occur simultaneously leading to a release behaviour which would be difficult to interpret. By varying the ion dose in the ion bombardment, the gas concentration can easily be varied without changing the purity of the specimen thus avoiding the disturbing impurities produced during reactor irradiation. By varying the energy of gas ions, the position of the gas with respect to the surface can be chosen thus enabling a separation of surface and bulk release processes. Moreover, the effect of radiation damage or specific impurities on release can easily be studied in double bombardment.

According to the method used and the conditions of introducing the gas traces it is possible to obtain samples in which the noble gas is distributed uniformly throughout the volume or located beneath the surface. The most common distribution profile (see Fig. 2) are:

- homogeneous distribution which is usually obtained either by neutron irradiation generating inert gas atoms in the bulk of the solid, or in natural minerals containing inert gases of radiogenic origin,
- distribution with a definite concentration profile beneath the surface (e.g. plane source, exponential, peaked with an exponential tails) obtained by ion bombardment, diffusion or recoil technique of labelling.

2.5. *Introduction of parent nuclides*

Trace amount of ^{226}Ra can be introduced into the sample by co-precipitation during the sample preparation from a solution or adsorption on the surface of the sample. ^{222}Rn is formed by spontaneous alpha decay of radium and can be introduced into the solid owing to the recoil energy (80 keV per atom). The above nuclear reaction which give rise to the radon nuclide, has also been used for the incorporation of the inert gas into the solid sample. Radon atoms penetrate several tens of nanometers, depending on the composition of the target materials.

3. State and diffusion of noble gases in solids

The solubility of noble gas atoms in inorganic solids is small. The inert gas atoms incorporated into solids are situated on the structure defects, such as vacancies, vacancy clusters, dislocations, grain boundaries and pores. The mobility of the inert gases in solids is strongly dependent on the structure and its changes. An important role in the gas migration is played by impurities of various kinds and by natural and artificially induced defects. The defects of the solid can serve both as traps and as diffusion paths for the noble gas.

Four diffusion mechanisms have been proposed to explain inert gas migration in solids [1].

- *Vacancy diffusion*. The inert gas atoms are assumed to occupy vacancy sites in the lattice and diffuse through either the cation or anion sublattice by jumping into appropriate adjacent vacancies.
- *Interstitial diffusion*. Inert gas atoms occupy interstitial sites in the lattice and diffuse by jumping into adjacent interstitial sites.
- *Interstitial diffusion plus trapping*. Inert gas atoms diffuse interstitially but may be trapped at defects in the lattice such as vacancies. If the binding energy to the defect is sufficiently large, the rate-controlling step in diffusion will be the release rate from the defect and the measured diffusion activation energy will involve both the defect binding energy and the energy of migration of the gas atom.
- *Mobile cluster diffusion*. Inert gas atoms associate with mobile vacancy clusters and move through the lattice with the cluster. Dissociation of the gas atom from the cluster, which immobilized the gas atom, may occur until another vacancy cluster diffuses to the lattice position adjacent to the gas atom.

4. Release of inert gas

Release of inert gas can be caused by a number of processes, such diffusion, release caused by the instability of the surface, annealing of lattice damage during heating, evaporation of surface layers, recrystallization or phase changes, chemical reactions of labelled sample, etc. A clear separation of various processes that contribute to the overall release is possible. These process were grouped by Matzke [10] into a system of stages.

- **Stage I** involves gas mobility at unusually low temperatures.
- **Stage IA** is due to gas fortuitously located in high mobility sites.
- **Stage IB** is due to annealing of the structural radiation damage, the most common form of which is radiation-introduced amorphous state.
- **Stage II** involves gas mobility at "normal temperatures", i.e. temperature similar to those of self-diffusion of the matrix atoms.
- **Stage IIA** is due to unperturbed mobility of single gas atoms.
- **Stage IIB** is due to interactions of gas atoms with radiation damage or pre-existing defects, or with other gas atoms.
- **Stage III** involves gas mobility at unusually high temperatures and is due to strong trapping of gas at pre-existing defects or in gas-filled bubbles.

Fraction release F or release rate J are most commonly measured in experiments where the inert gas release is studied. The heating at various temperatures for a definite time, so called isothermal step-heating or isochronal heating, or the heating in conditions of increasing temperature are usually employed.

4.1. Normal volume diffusion mechanism

The diffusion stage of the release is usually observed at temperatures when the self diffusion in the crystal lattice of solids takes place and when the inert gas is distributed in the whole volume of the sample. In this case the inert gas release can be described by the solution of Fick's laws by taking into account the respective initial and limit conditions and the geometrical form of the samples investigated [11]. The initial differential equation taking into account various geometrical shapes of the sample can be written in the form of Eq. (1)

$$\frac{\partial C}{\partial t} = D\frac{1}{r^{\nu}}\frac{\partial}{\partial r}\left(r^{\nu}\frac{\partial C}{\partial r}\right) \tag{1}$$

where $C(r,t)$ is the concentration of inert gas, t is time, D is the inert gas diffusion coefficient, r is the radial coordinate, $\nu = 0$ for a plate, cylinder or prism with impermeable sides, $\nu = 1$ for a cylinder or prism with impermeable bases (i.e., infinite cylinder), $\nu = 2$ for a sphere. Eq. (1) has to be solved at the limit conditions

$$C(L,t) = 0 \tag{2a}$$

$$\frac{\partial C(0,t)}{\partial r} = 0 \tag{2b}$$

$$C(r,0) = f(r) \tag{2c}$$

where L is the characteristic size of the elementary volume at the point where sample diffusion takes place, e.g., the half width of the plate or radius of the sphere or cylinder.

For homogeneous distribution of the diffusion gas in the volume of the sample $C(x,0) = C_0$ the solution of Eq. (1) under the limit conditions (2) results in the time dependence of the density J of the flux of inert gas release, in Eq. (3)

$$J = \frac{2(\nu+1)D}{L^2}\sum_{m=0}^{\infty}\exp\left(-\mu_{m,\nu}^2\frac{D}{L^2}t\right) \tag{3}$$

Where $\mu_{m,\nu=0} = (2m+1)\pi/2$, $\mu_{m,\nu=1} = q_m$, $\mu_{m,\nu=2} = \pi m$ and q_m are nuclei of the Bessel functions.

The existence of the temperature dependence of the diffusion coefficient causes more complicated mathematical expressions for the equation of the inert gas release flux J.

The temperature dependence of the diffusion coefficient is usually represented as

$$D = D_0\exp\left(\frac{-E_d}{RT}\right) \tag{4}$$

where D_0 and E_d are the pre-exponential factor and activation energy of inert gas diffusion, respectively, R is the molar gas constant, and T is temperature (in K).

In conditions of constant heating rate the temperature increase according to the relationship

$$T = T_0 + \beta t \tag{5}$$

where T_0 is the temperature of the onset of sample heating, β is heating rate (in K s^{-1}), t is heating time (in s). Then the time dependence of the diffusion coefficient can be described by Eq. (6)

$$D(t) = D_0\exp\left[-\frac{E_d}{R}(T_0+\beta t)\right] \tag{6}$$

The time dependence of the flux J of the inert gas release on constant heating rate of the sample can be obtained by replacement in Eq. (3) of D by $D(t)$ (see Eq. (6)) and D_t by the integral time τ_i which in given by

$$\tau_i = \int_0^t D(\tau)\,\mathrm{d}\tau = \int_{T_0}^{T} D(\theta)\,\mathrm{d}\theta \tag{7}$$

Under conditions of a linear temperature increase we can write

$$e\tau_i = \frac{D_0E_d}{\beta R}\left[-\frac{\exp(\tau)}{\tau} + E_i(\tau)\right]_{\tau=-E_d/RT_0}^{\tau=-[E_d/R(T_0+\beta t)]} \tag{8}$$

where

$$E_i(z) = \int_{-\infty}^{z}\frac{\exp(\tau)}{\tau}\,\mathrm{d}\tau$$

Finally, in the case of a uniformly labelled sphere with radius r_0, the flux J of the inert gas from the sample is expressed by Eq. (9)

$$J = \frac{2C_0SD_0}{r_0}\exp\left(-\frac{E_d}{RT}\right)\sum_{n-1}^{\infty}\exp\left(-\frac{n^2\pi^2\tau_i}{r_0^2}\right) \tag{9}$$

where S is surface area of the sample, the constant heating rate condition being supposed.

As it follows from Eq. (9) with conditions of linearly increasing temperature, the time dependence of the inert gas flux J can be represented by an asymmetric peak-like curve (see Fig. 3). The peak maximum temperature rises with the increase of the diffusion activation energy, radius of the grain and the sample heating rate. The decrease of the pre-exponential factor should also lead to an increase in the temperature of the peak maximum.

Cases of plane source and exponentially decreasing profile, linearly decreasing gas distribution, and peak distribution with an exponential tail were analysed by Kelly and Matzke [12]. The $J(T)$ curves for linearly

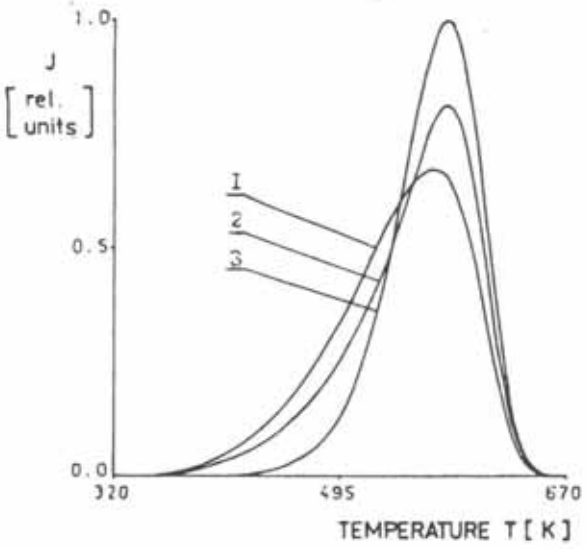

Fig. 3. Computed temperature dependences of the thermostimulated inert gas release during constant rate heating of samples of various shape, supposing various diffusion stages: curve (1) spherical sample, diffusion stage of gas release; curve (2) plate, diffusion stage of gas release; curve (3) kinetic stage of gas release. The values of E_d=20 kcal mol^{-1}, $\ln(K_0R/E_d = 23$ are assumed.

increasing temperature exhibit peaks, the maxima (T_m) of which are governed mainly by the value of the activation energy, E_d. The shapes of peaks depend markedly on the type of diffusion and on the heating rate β and the median or 50% range R_m.

The expression for E_d/T_m is

$$\frac{E_d}{T_m} = (A \pm 5) + 4.6\,\frac{\log_{10} T_m}{R_m^2 \beta} \tag{10}$$

where activation energy E_d is given in cal mole^{-1} and heating rate β in K min^{-1}. Constant A depends on the distribution profile and the diffusion type [1]. R_m is the median range of ions in units of atomic spacings a, which for single jump mechanism equals 1 and for a sphere is taken as radius r_0. The uncertainty ± 5 arises from the assumption of D_0 values. The range $D_0 = 3 \times 10^{-1} \pm 1$ cm^2 s^{-1} is obeyed in metal diffusion and also applies well to self-diffusion in the ionic crystals as alkali halides.

The widths of the peaks depends mainly on the character of the gas distribution. The narrowest one corresponds to a single jump mechanism, while a wider peak was obtained with a plane source, the width of the peak being increased with the median range R_m [13]. The expression for the width of a gas release peak under conditions of linearly increasing temperature, $T_{1/2}$ can be written is general form as follows

$$\frac{\Delta T_{1/2}}{T_m} = B - C\,\frac{\log_{10} T_m D_0}{R_m^2 \beta \cdot 0.3} \tag{11}$$

B and C are constants which depend on the geometry of samples.

4.2. Retarded gas release due to a trapping

Theoretical considerations suppose an ideal volume diffusion mechanism of the inert gas release. A large number of gas release experiments follows this ideal diffusion pattern. However, the larger part of the experimental work showed deviations, e.g. retarded gas release. An important role in the gas migration is played by impurities of various kind and by natural and artificially induced defects: vacancies, vacancy clusters, dislocations, grain boundaries and pores.

In the retarded gas release mechanism gas atoms are considered that migrate in the solid matrix via random walks that are interrupted by trapping into various imperfection existing in a material [14]. The sample is believed to contain the inert gas in two energetically distinguishable sites: in the continuous phase of the solid (i.e. "normal") and in the defect (i.e. "trapped") ones. Isolated point defects with an unlimited capacity are randomly distributed in the bulk of the solid. In the course of their random motion, inert gas atoms are trapped by the defects and are excluded for a definite time interval from the diffusion process. Mathematically, a trapping effect has been introduced in Fick's law by adding reaction between mobile gas atoms and stable distribution of traps [15,16]. The process, called "gas diffusion with reversible trapping", can be described by following differential equations:

$$\frac{\partial C_1}{\partial t} = D\frac{\partial^2 c_1}{\partial x^2} - k_1 N_2 c_1 + k_2 N_1 c_2 = D\frac{\partial^2 c}{\partial x^2} - k_1^* c_1 + k_2^* c_2 \tag{12a}$$

$$\frac{\partial C_2}{\partial t} = k_1 N_2 c_1 - k_2 N_1 c_2 = k_1^* c_1 - k_2^* c_2 \tag{12b}$$

where C_1 and C_2 are the concentrations of the diffusion agent in the diffusion channels and traps, respectively, N_1 and N_2 are the number of states 1 and 2, k_i is the rate constant for the passage of inert gas atoms from one energy state to another, D is the undisturbed diffusion coefficient, and

$$k_1^* = k_1 N_2 \text{ and } k_2^* = k_2 N_1$$

The first-order chemical reaction kinetics is used for describing the trapping of gas atoms by the matrix and subsequent release of the gas.

The trapping reaction is

$$\text{defect} + \text{gas atoms} \underset{k_2}{\overset{k_1}{\rightleftarrows}} \text{defect} = \text{atoms complex (immobile)} \quad (13)$$

A quasi-chemical equilibrium is shifted to the left-hand side at high temperatures, favouring movement of the gas to its mobile state and vice versa. The equilibrium constant of the trapping reaction is

$$K_H = \frac{n_2}{n_1} = \frac{k_1 N_2}{k_2 N_1} = \frac{k_1^*}{k_2^*} = \frac{c_2}{c_1} = K\frac{N_2}{N_1} \quad (14)$$

where $K = k_1/k_2$

The inert gas flow from the spherical or plate-like sample has been considered in the mathematical modelling experiments [1].

An important special case of the model is given when the trapping reaction has reached its thermal equilibrium. Differential Eqn. 12 reduces to the simple Fick's type, with D_{app}, which is smaller than D for undisturbed diffusion. If the local equilibrium is reached during the experiment ($k_1^* C_1 = k_2^* C_2$), the observed diffusion coefficient for the mobile gas, D_{app} by the following expressions:

$$\frac{\partial c}{\partial t} = \frac{D}{(1+K_H)}\frac{\partial^2 c}{\partial x^2} = D_{app}\frac{\partial^2 c}{\partial x^2} \quad (15a)$$

where,

$$D_{app} = \frac{D}{1 + K\phi_2/\phi_1} = \frac{D}{1+K_H} \quad (15b)$$

These results are derived by considering the equilibrium distribution of gas atoms between normal sites and traps. The expressions for the diffusion coefficient are correct if this equilibrium is established rapidly compared with the rate of diffusion of the gas out of the solid, and this condition is satisfied in many experiments. Temperature dependences of the effective diffusion coefficient of inert gases in highly disordered media obtained by mathematical modelling are given in [17].

4.3. A mobile cluster diffusion mechanism of inert gas

Matzke [18] was the first to suggest that inert gas atoms could possibly associate with mobile defect clusters and move with clusters through the lattice. The gas atoms may periodically dissociate from the clusters, and become trapped in the lattice. These diffusion models consider the transport of an atom from a solid with two diffusion coefficient: D_1 and D_2 ($D_2 \gg D_1$). The diffusion coefficient D_1 relates to the simple inert gas diffusion. The diffusion coefficient D_2 relates to gas-defect cluster diffusion. When a gas atom, diffusing in a solid, is exchanged between two diffusion streams, so-called dissociative diffusion takes place [19].

The system of the differential equations describing one-dimension diffusion in a planar sample with a thickness l, when a reversible quasi-chemical reaction of the first order takes place between gas atoms and mobile cluster, is given by the following differential equations:

$$\frac{\partial C_1}{\partial t} = D_1\frac{\partial^2 c_1}{\partial x^2} - k_1^* c_1 + k_2^* c_2 \quad (16a)$$

$$\frac{\partial C_2}{\partial t} = D_2\frac{\partial^2 c_2}{\partial x^2} + k_1^* c_1 - k_2^* c_2 \quad (16b)$$

where C_1 and C_2 are the concentrations of the inert gas atoms in dissolved form and in the complex form with mobile defects.

In the absence of local equilibrium the system of the differential Eqn. 16 should be solved using the general initial and boundary conditions. The unidirectional flux J_x is given by the linear combination of two Fick's-law contributions:

$$J_x(T) = -D_1(T)\frac{dc_1}{dx} - D_2(T)\frac{dc_2}{dx} \quad (17)$$

If the local equilibrium is reached during the experiment ($k_1^* C_1 = k_2^* C_2$), the observed diffusion coefficient for the mobile gas, D_{app}, can be written:

$$D_{app} = \frac{D_1 + K_H D_2}{1 + K_H} = \frac{D_{10}\exp(-E_1/RT + H_{H0}D_{20}\exp[-(E_2 - E_{KH})/RT]}{1 + K_{H0}\exp(E_{KH}/RT)} \quad (18)$$

where $D_{1,0}$, D_{20}, E_1 and E_2 are the respective prexponential factors and activation energies, and K_H is the equilibrium constant of the inert gas exchange between the two channels (see Eq. (14)).

Like the trapped interstitial model, the mobile cluster diffusion qualitatively explains most of the features in inert gas diffusion experiments.

4.4. *"Single-jump" diffusion mechanism: the desorption of gas as first order kinetics reaction*

The kinetic stage of the inert gas release is usually observed after long diffusion times, i.e. when the majority (>80%) of inert gas has been released. However, in many cases the kinetic stage of inert gas release can be considered as the beginning of the TIGRA-experiment [11]. This is for e.g. the case of inert gas desorption from solid surfaces, the inert gas diffusion in highly defected solid media (e.g. meteorites and natural minerals) the inert gas diffusion from the surface layers of solids labelled by ionic bombardment or nuclear reactions, the case of solids with large surface area (e.g. zeolites) and when intense solid state processes take place during the heating of the sample (e.g. annealing of defects, phase transitions, solid state reactions, etc.).

In the kinetic stage, the inert gas release is almost independent on the initial concentration profile of the inert gas in the solid sample, the geometrical shape and size of the sample investigated; usually it takes place at temperatures considerably lower than the volume diffusion of inert gases in the respective solids.

This behaviour can be explained by the "single-jump" diffusion model considering that for the release of inert gas atoms a small number (less than 100) of gas-atom jumps in the lattice is sufficient. Considering the kinetic stage of inert gas release, the classical diffusion equation (see Eq. (1)) can be substituted by the equation of the first order chemical reaction in Eq. (19)

$$\frac{dC}{dt} = -K_d C \quad (19)$$

where $K_d = \pi^2 D/d^2$, d being the length of diffusion jump, C is the number of the inert gas atoms which are present in the sample at time t.

The inert gas flux J from the sample heated at a constant rate is given by Eq. (20).

$$J = C_0 K_0 \exp\left(-\frac{E_d}{RT}\right)\exp\left\{-K_0 t \exp\left(-\frac{E_d}{RT}\right)\right\} \quad (20)$$

In Fig. 3 the temperature dependences of the thermostimulated inert gas release during constant heating of spherical samples or plates are demonstrated. In calculations, the volume diffusion mechanism (curves 1 and 2) and the single jump diffusion mechanism (curve 3, Fig. 3) were considered. The main influencing factors are the geometrical shape of the grains and the diffusion mechanism of the inert gas. Supposing the same parameters of the inert gas diffusion, the size of the samples and the volume diffusion mechanism of inert gas, curve 1 in Fig. 3 results for spherical samples, with the maximum at a lower temperature than in the case of plates or samples of other shapes (Fig. 3, curve 2). When "single-jump" diffusion is considered, the inert gas release curves are more symmetric and the peak is sharper (Fig. 3, curve 3) than in the curves of the volume diffusion mechanism, and are independent of the shape of the sample.

5. Analysis of the TIGRA curves

5.1. *Thermostimulated inert gas release as influenced by the spectrum of bond energies between the inert gas and the defect sites in the solid*

In the critical review [11] a solid sample labelled by an inert gas which is trapped in various defect sites, was supposed. It was considered that N_i is the number of sites of ith type and that the sample contains m types of defects [20].

For characterization of the solids labelled by inert gas before the sample heating, the energy spectrum $N(E)$ of the defect sites, and the energy spectrum $n(E)$

of the inert gas in the solid were used. In the case of total occupation of the defect sites by the inert gas, the spectra $N(E)$ and $n(E)$ were considered as identical.

The inert gas release can be described by a first-order reaction mechanism, determined by the activation energy, E_i, then the time dependence of the inert gas flow $J(t)$ from the sample heated at constant heating rate can be expressed

$$J = \frac{\mathrm{d}\theta_i^*}{\mathrm{d}t} = K_{0,i} \exp\left(-\frac{E_i}{RT}\right)\theta_i^* \tag{21}$$

where θ_i^* is the dimensionless expression for the number of inert gas atoms located on ith type sites, normalized on the total number of the defects N where $N = \sum_{i=1}^{m} N_i$.

The total inert gas flow J from sample is

$$J = \frac{\mathrm{d}\theta}{\mathrm{d}t} = \sum_{i=1}^{m} K_{0,i} \exp\left(-\frac{E_i}{RT}\right)\theta_i^* \tag{22}$$

where $\theta = \sum_{i=1}^{m} \theta_i^* = 1/N \sum_{i=1}^{m} N_i$ is the complete occupation of the sites by the inert gas.

The term of $\phi_i = N_i/N$ equalling the proportion of the potential sites of the ith type normalized to the total number of defects of the ith type was introduced [20]. Eq. (22) can be written using the parameter ϕ_i as follows

$$\frac{\mathrm{d}\theta}{\mathrm{d}t} = \sum_{i=1}^{m} K_{0,i} \exp\left(-\frac{E_i}{RT}\right)\phi_i\theta_i^* \tag{23}$$

In the case of the continuous spectrum of the activation energies of inert gas release, for inert gas flow J

$$J = \frac{\mathrm{d}\theta}{\mathrm{d}t} = -k_{\mathrm{ef}}\theta = \int_0^{\theta} k_0(\theta^*) \exp\left(-\frac{E(\theta^*)}{RT}\right)\mathrm{d}\theta_i^* \tag{24}$$

and after substituting $\mathrm{d}\theta^* = \theta\,\mathrm{d}\phi$ we obtain

$$J = \frac{\mathrm{d}\theta}{\mathrm{d}t} = -\int_0^{1} k_0(\phi) \exp\left(-\frac{E(\theta^*)}{RT}\right)\theta(\phi)\,\mathrm{d}\phi \tag{25}$$

The experimental conditions of the constant heating rate are taken into account. The solution of Eq. (23) can be written in the form

$$J(t) = \sum_{i=1}^{m} \theta_{0,i} k_{0,i} \exp\left(-\frac{E_i}{RT}\right) \exp(\tau_i) \tag{26}$$

where the integral time $\tau_i = (k_{0,i}E_i/\beta R)\{-[\exp(\xi)/\xi] + E_i(\xi)\}$ (see Eq. (8)).

In order to analyse the temperature dependences of E_{ef}, the values of the effective diffusion constant were first determined at every point on the experiment curve $J(t)$. The effective diffusion constant k_{ef} can be expressed

$$k_{\mathrm{ef}} = \frac{J(T)}{\theta T} = \frac{J(T)/F}{1 - 1/F \int_{T_0}^{T_F} J(T)} \tag{27}$$

where $F = \int_{T_0}^{T_F} J(T)$ is the area of the peak of the TIGRA curve and T_0 and T_F are the onset and final temperature of the heating respectively. The calculated Ink_{eff} values were plotted against $1/T$ at every point on this curve; and the activation energy E_{ef} and $k_{0,\mathrm{ef}}$ were evaluated. Subsequently, the temperature dependences of the plots E_{ef} against T and $k_{0,\mathrm{eff}}$ against T were constructed. On the basis of these plots, the spectrum of the activation energy of the inert gas release was investigated. The principles are pointed out below:

1. when the spectrum consists of a single activation energy, the plot of E_{ef} against T is linear and parallel to the x-axis; and
2. when the spectrum consists of several values of activation energy, the plot of E_{ef} against T is non-linear decreasing when the energy values are difficult to distinguish, and has a minimum when the energy values are clearly distinguished.

The application of this method in the analysis of the model TIGRA curves is demonstrated in Figs. 4 and 5 and Fig. 6. It was assumed that the energy spectrum consists of two discrete lined E_1 and E_2, where $E_1 < E_2$.

In Fig. 4 schemes of the energy spectra $n(E)$ of the defect sites in the solids considered during the mathematical modelling are given. The spectrum is characterised by two activation energy values E_1 and E_2, assuming the same occupation of the respective defect sites by the inert gas($\theta_1 = \theta_2$). The spectra shown are assumed to have the same E_1 but different values of E_2.

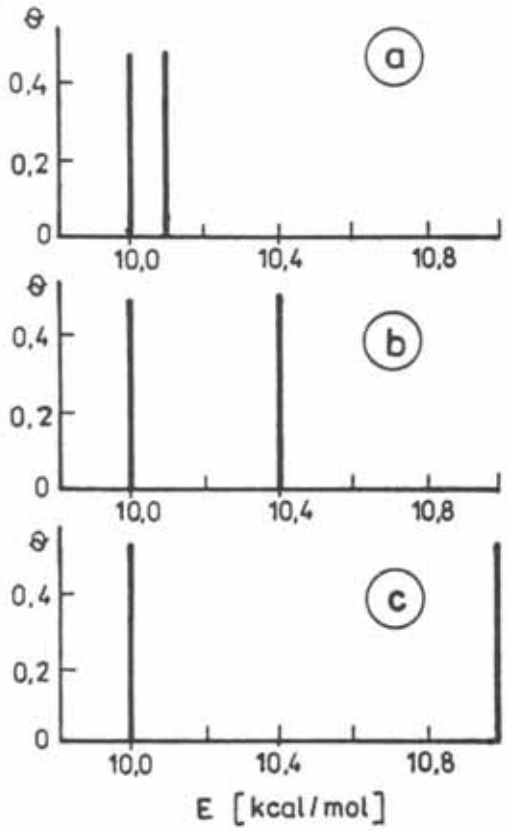

Fig. 4. Schematic diagrams of the discrete energy spectra $n(E)$ of the solid state defect sites taking part in the inert gas diffusion. Two different values E_1 and E_2 of the effective activation energy of inert gas diffusion and the equal occupation of the defect sites by the inert gas $\theta_1=\theta_2$ are supposed:(a) E_1= 10.0 kcal mol^{-1}, E_2=10.1 kcal mol^{-1}(b)E_1=10.0 kcal mol^{-1}, E_2=10.4 kcal mol^{-1}, and (c) E_1 =10.0 kcal mol^{-1}, E_2=11.0 kcal mol^{-1}.

In Fig. 5 typical curves of the temperature dependences of the inert gas release from solids are demonstrated. It is obvious from Fig. 5 that the dependences are single peaked curves, irrespective of whether one or two activation energy values are considered in the discrete spectrum. A higher symmetry was observed in the case where the energy spectrum has two lines. However, when the method of the analysis of temperature dependences, lnk_0 versus T and E_{ef} versus T, was used, the influence of both values of activation energy in the spectrum was found (see Fig. 6). In Fig. 6, the influence of energy lines in the spectrum differing by only 1% can be seen. A difference in the energy lines of 4% is more obvious.

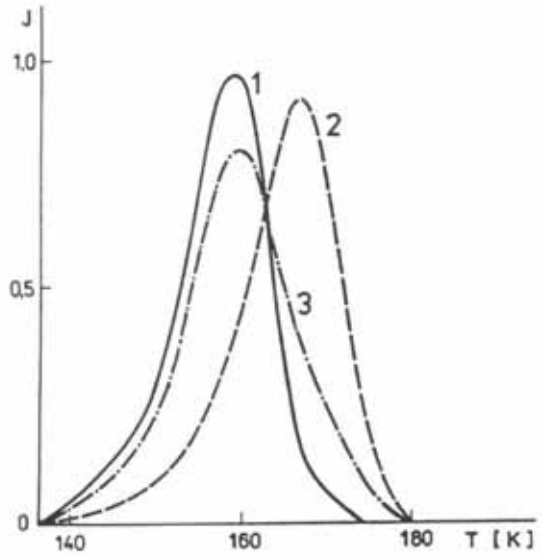

Fig. 5. Model curves of the temperature dependences of the thermostimulated inert gas release (TIGRA curves) for the selected cases of the discrete energy spectra of the single energy value E_1 = 10.0 and 10.5 kcal mol^{-1}, respectively: curve 3 corresponds to the spectrum characterized by two discrete energy values E_1= 10.0 kcal mol^{-1} and E_2=10.5 kcal mol^{-1}. In the modelling, the heating rate 2.0 Ks^{-1} and the pre-exponential factor 10^{13} s^{-1} were considered.

5.2. *Influence of the labelling conditions on the character of the TIGRA curves*

In the case of the diffusion technique of labelling the shape of the TIGRA curves depends considerably on the conditions of the sample labelling, e.g. the inert gas pressure and the duration of the diffusion labelling of samples.

A solid sample containing several defect sites characterized by the discrete-energy Spectrum $N(E)$ was considered in [21]. When such a solid is maintained under high inert-gas pressure, the defect sites will become occupied by the gas. Supposing that the defect sites are equally accessible for the inert gas, the inert gas will first be trapped on the sites of maximum energy. The distribution of the gas between the defect sites is either given by the Boltzman distribution function (in the case of partially occupied defect sites), or by the Fermi–Dirac distribution (in the case of the complete occupation of the defect sites). When the pressure of the inert gas is increased, the energy

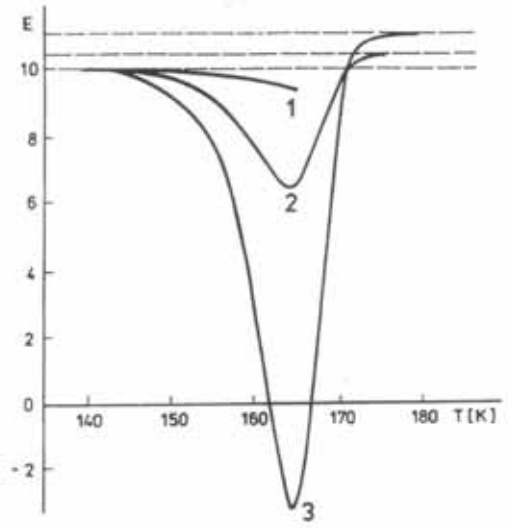

Fig. 6. Tempereature dependences of the effective activation energy E_{ef} of the inert gas diffusion calculated at every point of the model TIGRA curves corresponding to the discrete energetic spectrum characterized by Fig.4 (curves 1–3 correspond to the schemes (a)–(c) respectively).

spectrum $n(E)$ of the inert gas located at the defects is similar to the energy spectrum $N(E)$ of the defect sites.

When the function $\phi(E)$ is to be determined from the TIGRA measurements, the experiments must be performed under the conditions of complete occupation of the defect sites by the inert gas. Supposing that the inert gas adsorption at every site is controlled by the Laangmuir law, the amount of the inert gas located at the defect sites of ith type with energy E is given by equation:

$$\theta_i(E) = \frac{n_i}{n_{i,\infty}} = \frac{K_i(E)p}{1 + K_i(E)p} \tag{28}$$

where $n_{i,\infty}$ is the maximum capacity of the ith type defect of the inert gas. K_i is the equilibrium constant with respect to the defect site, and p is the partial pressure of the inert gas. The relationship $n_i = K_i p$ results from the Henry law. At low-pressure values the dependence of θ on p is linear, independent of p.

The total amount, n_i of inert gas located in the solid sample is

$$n = \int_{E_{min}}^{E_{max}} n(E)\,\mathrm{d}E \tag{29}$$

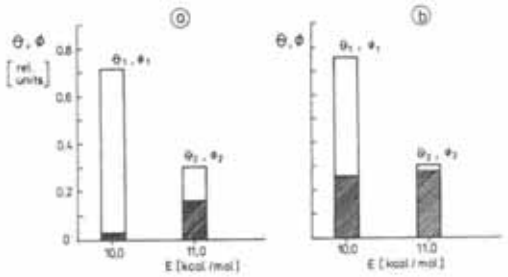

Fig. 7. Schematic diagrams of the discrete-energy spectra of the defect sites $\phi(E)$ and the degree of occupation of the defect sites by inert gas introduced at: (a) labelling pressure p=0.5 relative units; and (b) labelling pressure p = 10 relative units. The effective activation energies E and corresponding degrees of occupation of the defect sites used are: E_1=10 kcal mol^{-1},ϕ=0.7 and E_2=11 kcal mol^{-1},ϕ=0.3.

where E_{min} and E_{max} are the limits of the energy spectrum $N(E)$ of the defect sites.

The schemes of the discrete-energy spectra $\phi(E)$ of the defect site and of the spectra of their occupation $\theta(E)$ under different inert gas function $\phi(E)$ and $\theta(E)$ for a single solid sample may differ substantially.

Fig. 7 illustrates schematically two discrete-energy spectra characterized by the energies E_1 and E_2 ($E_1 < E_2$) and the degrees of occupation ϕ_1 and ϕ_2. At low pressure the relative occupation (θ_1 and θ_2) of the energy sites E_1 and E_2 is $\theta_1 < \theta_2$, at medium pressures $\theta_1 \cong \theta_2$ and only at sufficiently high pressures does θ_1 become higher than θ_2. In practice this means that as the inert-gas pressure is increased, the defect sites of potential energy E_2 are occupied first. The redistribution of the inert-gas atoms between the potential-energy sites E_1 and E_2 depends on the temperature dependence of the equilibrium constant K. The defect sites of potential energy E_1 usually (at the low pressures used for sample labelling) contain a much lower amount of inert gas than do the defects of potential energy E_2, the occupation of the defect sites of energy E_1 takes place.

It is obvious that the inert-gas spectrum $\theta(E)$ reflected by the TIGRA curves may differ substantially as the partial pressure of the inert gas is changed. If this fact is neglected, substantial errors can be made in the interpretation of the TIGRA curves.

Fig. 8 shows the TIGRA curves computed for linearly rising temperature in the cases of the discrete defect-site spectra shown in Fig. 7. At low partial

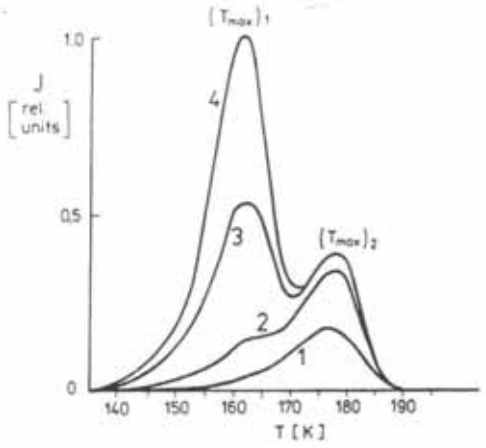

Fig. 8. The model TIGRA curves computed for the case of the defect sites of two discrete energy lines (E_1 =10 kcal mol^{-1}, ϕ_1 = 0.7 K= 0.01; and E_2=11 kcal mol^{-1}, ϕ_2 =0.3, K=1) and different partial pressures during sample labelling. The pre-exponential factor K_0= 10^{13} s^{-1} and the linear heating rate β=2 Ks^{-1} were supposed. Curves 1–4 correspond to relative partial pressures of (in relative units): 1, 10, 100 and saturation gas pressure respectively.

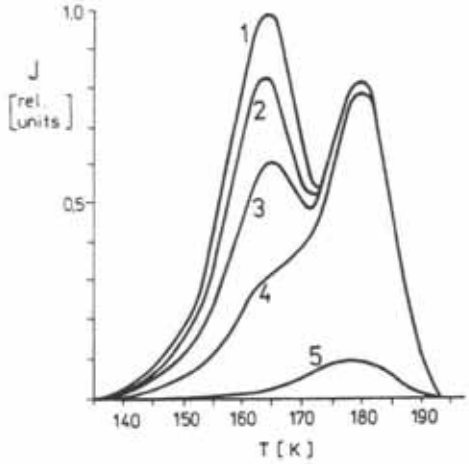

Fig. 9. Model TIGRA curves for the linear heating rate β=2 Ks^{-1} and the partial outgassing of samples at 140 K. The defect sites characterized in Fig.7 were assumed. Curves 1–5 correspond to preliminary outgassing durations of: 0, 5, 6, and 11 relative units, respectively.

pressures the one-peak TIGRA curve result, as expected, in the energy of the defect sites determining the maximum J_{max}.

When the partial pressure of the inert gas during labelling is increased, the height of the $(J_{max})_2$ peak rises, in correspondence with the Langmuir isothermal curve. In Fig. 8, curve 3, it is shown that at a relative partial pressure of $p = 100$ during sample labelling, the maximum height of $(J_{max})_2$ is attained whereas the height of $(J_{max})_1$ increases.

At the high pressures of inert gas used, $(T_{max})_1$ becomes most significant in the TIGRA curve. The importance of the sample labelling conditions on the TIGRA model curves has been shown here. The results have been used for the assessment of the functions $\theta(T)$ and $\phi(T)$ from the experimental TIGRA curves.

5.3. *Influence of preliminary sample thermal treatment on the TIGRA curves*

The amount of inert gas located at the defect sites of solids also depends on the preliminary thermal treatment of the solid samples. The solid sample characterized by the discrete-energy spectrum shown in Fig. 7 can be obtained by the diffusion technique of labelling at partial pressures which ensured the complete occupation of the defect sites by the inert gas. The preliminary thermal treatment caused the partial outgassing of the labelled sample. The choice of a suitable temperature and duration of the thermal treatment makes it possible to influence the shape of the TIGRA curves. Therefore, the determination of the energy spectrum of the inert gas labelling can be simplified.

Fig. 9 shows the model TIGRA curves computed for the samples whose energy spectra are given in Fig. 7, and for preliminary sample outgassing at 140 K assuming various time intervals for the sample outgassing. It can be seen from Fig. 9 that the height of the first peak diminished with increasing duration of the thermal treatment. When the treatment is sufficiently long, the first peak disappears completely and the second peak diminishes substantially.

6. Measurement of inert gas release

The apparatus for TIGRA consists of several components designed to ensure the detection of inert gas, and to provide sample heating and temperature control. In addition, the instrument supplies the carrier gas

with flow stabilisation, and measures the gas flow and complementary parameters.

During an analysis, the carrier gas (air, nitrogen or another suitable gas) carries the inert gas released by the sample in the vessel (situated in a furnace) into a detector for the inert gas. For example, to measure the α-activity of Rn, a scintillation counter, ionisation chamber or semiconductors can be used. On the other hand, all β-activity measurements involving Kr, Xe and Ar are made by Geiger–Muller tubes. Gamma-active gases can be measured by a γ-spectrometer. The stable nuclides of inert gases are measured by a mass spectrometer. To ensure optimum conditions for a direct comparison of TIGRA data with results obtained by other thermoanalytical methods, devices were constructed to provide simultaneous measurement of additional parameters [1].

7. Evaluation of TIGRA experimental data

The computer software for mathematical modelling of thermostimulated inert gas release kinetics, and for evaluation of experimental data of TIGRA methods represents an important part of modern thermal analysis. The computer is used in the control of TIGRA equipment operation and in the evaluation of the results. The TIGRA of composites, mixtures, natural rocks and other materials as well as multistage diffusion processes accompanied by solid-state reactions make mathematical description rather complicated, which can be solved by means of computers.

A set of computer programmes called DIGS (diffusion of inert gas in solids) for the statistical treatment and interpretation of the results of various methods used for the investigation of transport properties of solids was designed [22–25]. Following parameters were considered:

- the gas concentration distribution along the width of the sample,
- the quantity of the gas in the solid,
- the quantity of the inert gas in gaseous phase,
- the gas fluxes at the output of the sample.

Various geometrical shapes (sphere, cylinder, plate) can be taken into account and diffusion coefficients depending on time, concentration and coordinates of the sample can be evaluated. Other diffusion parameters can be determined and the fitness of adequate diffusion models can be verified. A bank of general diffusion models has been organized on the basis of both analytical and numerical solutions of diffusion cases. In the bank of experimental data the standard interface for the input of experimental data is used.

The set of the programmes involves four parts which give following possibilities:

- preliminary treatment of experimental results,
- evaluation of the results on the basis of the classical diffusion model,
- choice of a more suitable phenomenological diffusion model,
- choice of a suitable physical diffusion model.

7.1. Testing the TIGRA apparatus

The TIGRA apparatus should be tested in order to estimate the distortion effect of the apparatus on the experimental curve. The testing consists of measuring the apparatus response to a short impulse of the gas. The resulting apparatus response $\phi(t)$ is usually normalized with respect to the total amount of the inert gas; true form of the experimental curve can be obtained by solving the Fredholm equation of the first order

$$f(t) = \int_0^t \psi(t-\tau)^* y(\tau)\,\mathrm{d}\tau \tag{30}$$

where $f(t)$ is the experimentally recorded curve, $y(t)$ is the true curve, $\psi(t)$ is the response of the apparatus to the short-time pulse.

7.2. Reconstruction of "non-distorted" TIGRA curves

Fig. 10 shows the results of the reconstruction of the TIGRA curve of a polypropylene film of thickness 100 μm, labelled by radon by a diffusion technique [26]. The TIGRA curve was measured during heating of the labelled sample at a constant rate of 4°C min^{-1}, over the temperature range from −196 to 400°C. As can be seen from curve 1, Fig. 10 which shows apparatus response to the "one second pulse", the

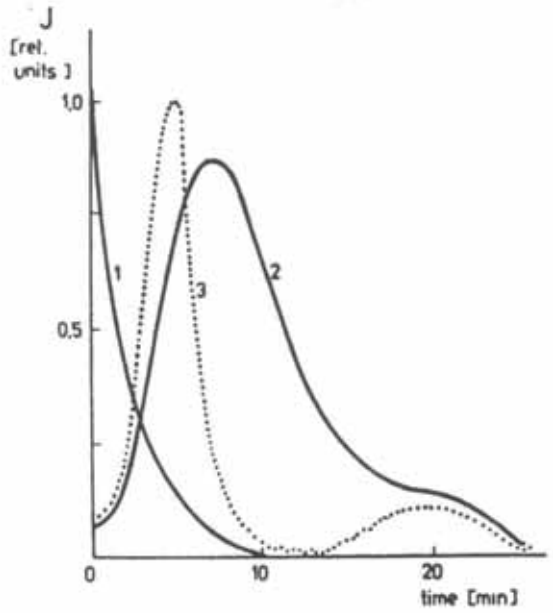

Fig. 10. The reconstruction of the experimentally obtained TIGRA curve of a polypropylene foil in the temperature range from −196 to +400°C (heating rate 4 min^{-1}) which was labelled with ^{222}Rn: curve (1)-the apparatus response to the "one second pulse", curve (2) - the experimentally obtained TIGRA curve; curve (3)-the reconstructed TIGRA curve.

apparatus may cause a significant distortion of the TIGRA curve, in this case mainly due to the rather high value of the time constant τ_i of the count-rate meter. The experimentally obtained TIGRA curve (Fig. 10, curve 2) exhibits a symmetrical form which could be ascribed to the inert gas release obeying first order release kinetics with a spectrum of activation energies.

However, as it follows from the reconstructed curve (Fig. 10, curve 3) the true form of the TIGRA curve is characterized by two effects, the first corresponding to the gas release controlled by first order kinetics with a single value for activation energy of 48 kJ mol^{-1}. On the basis of the reconstructed (true) TIGRA curve it can be stated that in the polypropylene foil sample, which has been prepared under a pressure of 100 atmospheres, radon atoms are situated in both amorphous and crystalline phases. These phases are characterized by different diffusion resistances, 84 and 126 kJ mol^{-1}, respectively. From the amount of inert gas release in the respective release processes it followed that in the amorphus phase about 80% of Rn, and in the crystalline phase about 20% of radon can be found.

7.3. *Determination of the inert gas diffusion parameters*

After the reconstruction of "true", non-distorted experimental curves the diffusion parameters can determined. The task of the treatment of experimental diffusion data can be substantially simplified when using functional scales which give the possibility of linearizing non-linear dependences between the parameters investigated. There exists a possibility to construct special diffusion scale sheets by means of which the linearisation of the non-linear dependences can be made directly and simply. For every technique used in TIGRA a functional scale was designed [11]. The diffusion parameters and errors of their determination can be evaluated by the least squares method.

The experimental curves of the thermally stimulated diffusion in normal scale and in the functional

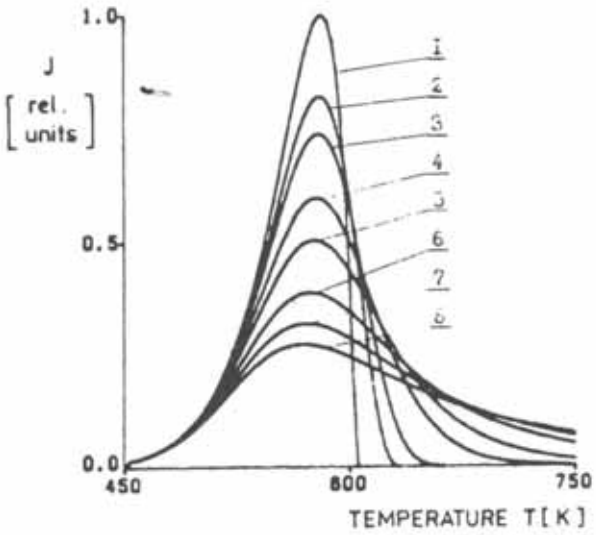

Fig. 11. Temperature dependences of TIGRA influenced by the inert gas trapping in the lattice of the solid. Differential diffusion equation is expressed as follows: $J(t) = K_0 C^n \exp(-E_d/R(T_0 + \beta t))$ where n is the formal order of reaction. The following order n of reaction mutual interactions between inert gas and lattice traps are considered, curves 1–8, respectively: n= 0.5, 0.8, 1.0, 1.5, 2.0, 3.0, 4.0, 5.0 (a) Normal scale (b) Functional scale.

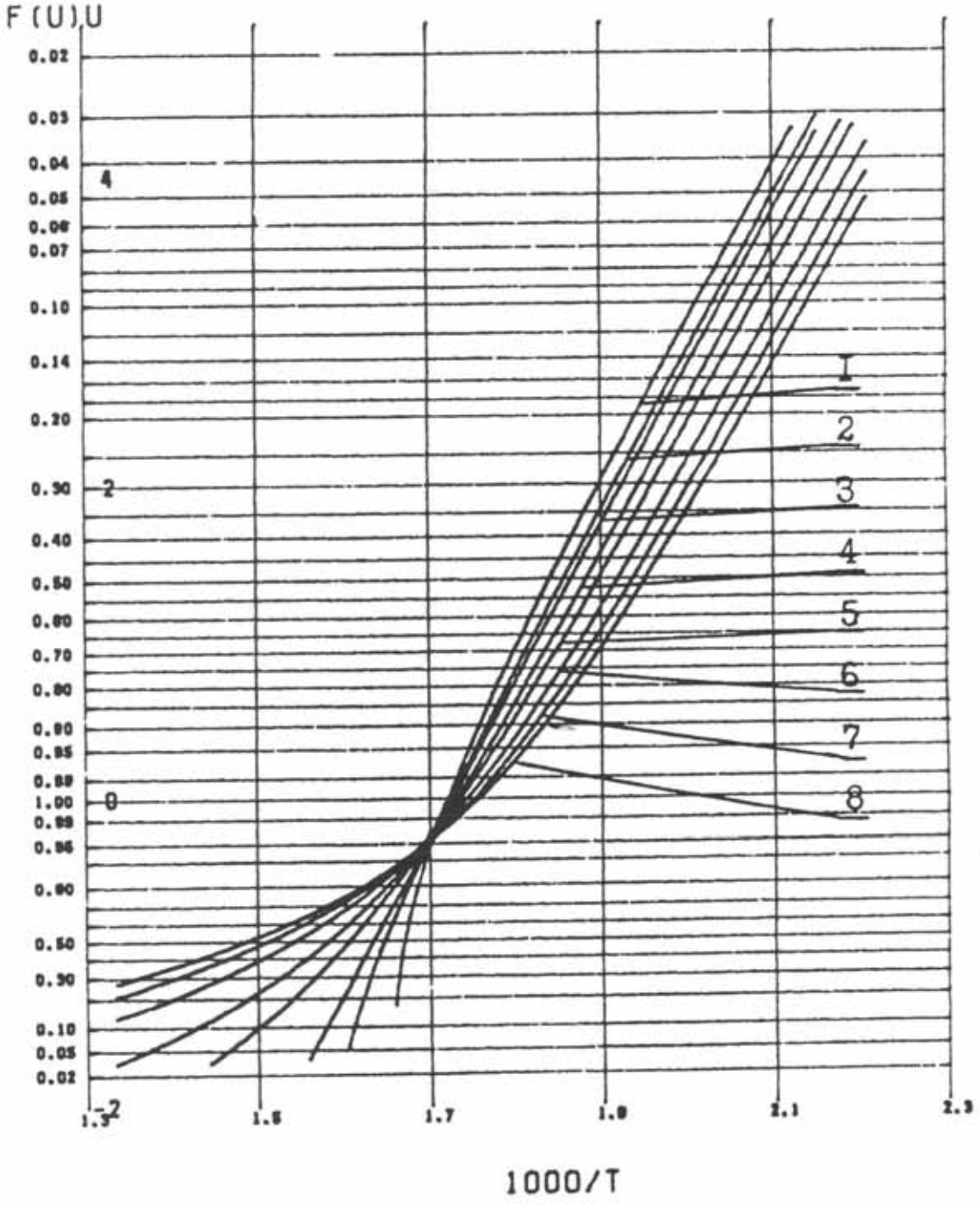

Fig. 11. (Continued).

scale are represented in Fig. 11 (a) and (b), respectively. In this way the initial peak-shape temperature dependence of the inert gas release is transformed to a linear dependence. There are several advantages of this simple method of treatment of diffusion experimental data. The linearized dependences of inert gas release enabled us to calculate easily the diffusion parameters using all points of the TIGRA curve. The suitable diffusion model to be used for the construction of the inert gas release curve can be estimated according to the correlation coefficient value. The most suitable diffusion model is the one where the corresponding correlation coefficient is close to unity.

In the case that the experimental data treated so far do not correspond to the model of classical diffusion, another more adequate diffusion model has to be chosen for the determination of the diffusion coefficient. The basic expressions necessary for the computer treatment are stored in a special bank of phenomenological diffusion models. The choice of an adequate diffusion model is made by a step-wise trial of various models, starting from a simple to more complicated ones. In the bank of phenomenological models analytical and numerical solutions of diffusion equations are stored, taking into account irreversible and reversible chemical reactions of the 1st and 2nd order between the gas and traps in the solid, various cases of parallel diffusion, diffusion taking into account the exchange of diffusing gas between the diffusion channels, etc. In solutions to the diffusion equations various concentration profiles of the gas in the solid, various concentration and time dependences of the diffusion parameters, etc. are considered. The choice of an adequate phenomenological model of diffusion is made by means of standard methods of mathematical statistics. A diffusion model is considered to be adequate when the difference between the experimental curve and the theoretically constructed curve corresponds to the normal distribution, and no drift of residues is observed.

In some cases the analysis of the experimental curves did not give us a possibility for determining the diffusion mechanism. In these cases dependences of the effective diffusion parameters on temperature, inert gas partial pressure, size of the sample and other parameters should be investigated.

8. Examples of TIGRA application

A number of authors in the past years used the Evolved Gas Analysis measuring the release of inert gases from solid samples. Although the inert gas release measurements carried out by various authors differed, a high sensitivity of the method to fine changes in the solid materials, phase and structure changes was observed. Results of additional measurements, such as electrical conductivity, DTA, TG, dilatometry, X-ray diffraction patterns, etc, were used in the interpretation of the EGA results.

In this part of the paper we shall demonstrate the high sensitivity of the EGA to various processes taking place during thermal treatment of different materials. It should be mentioned that methods of computer treatment of the experimental data developed in the recent years (and described in this paper) were not used in the demonstrated cases. Nevertheless, the demonstration of the results should promote interest in the TIGRA applications.

8.1. Diagnostics of the defect state

Inert gas diffusion parameters evaluated from TIGRA measurements reflect the mobility of noble gases in the solids, which can be used in the determination of the defects in the solids. Inert gas atoms incorporated into solids are situated on the natural and/or artificial defects produced, for example, by ion bombardment, neutron irradiation or mechanical treatment. The release of the inert gases on sample heating reflects the thermally stimulated processes, i.e. diffusion, annealing of defects, etc. It was shown that the mobility of inert gas atoms in the ionic crystals differs in various crystallographic directions, owing to the channelling effect. The mobility of the inert gases (the activation energy) can be used as a parameter characterising the defect state of an ionic crystal lattice and may cause the formation of the metamict phase.

Kornelsen and Sinha [27] presented the results indicating differences in the mobility of neon, argon, krypton and xenon ions in a tungsten single crystal. The temperature dependences of the Ne, Ar, Kr, and Xe release from W single crystal introduced in W single crystal by ion implantation at the energy of 600 eV and the dose of 5×10^{12} ion cm^{-2}, in

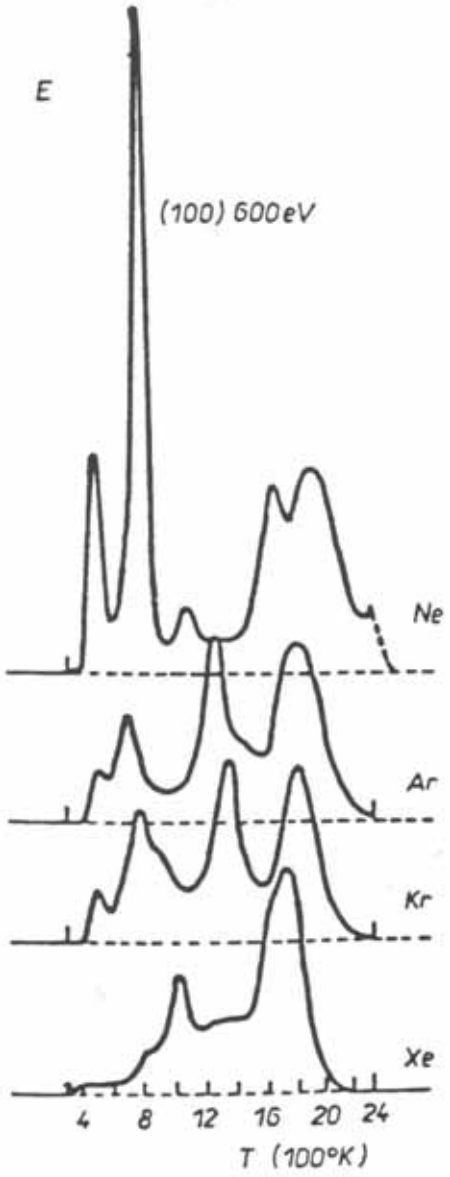

Fig. 12. Temperature dependences of Ne, Ar and Xe release from tungsten single crystal. The inert gases were incorporated by ion bombardment at the energy of 600 V and the dose of 5×10^{12} ions cm^{-2} in the crystallographic direction <100>.

the crystallographic direction ⟨100⟩ are given in Fig. 12. The results of inert gas release from other materials, such as Si, Ge, GaAs and SiC are given in [28].

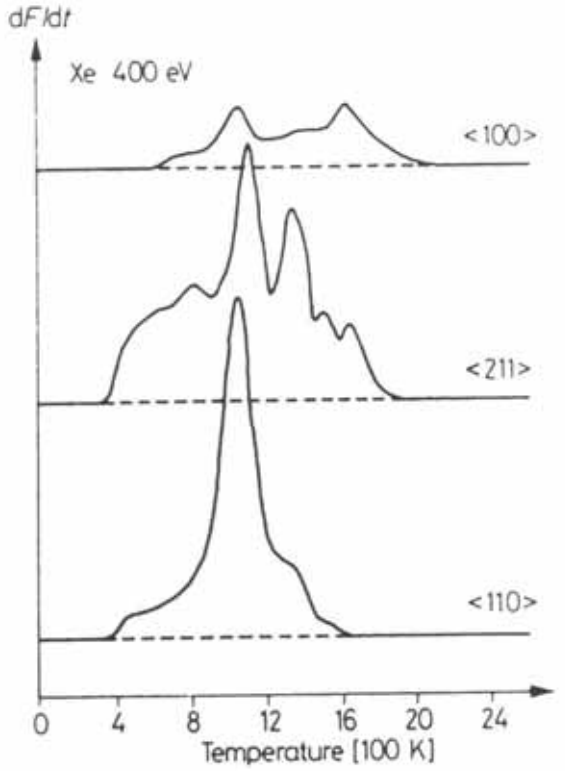

Fig. 13. Xenon release from the three different faces of single tungsten crystals after 400 eV Xe bombardment.

8.2. *Crystal orientation effects.*

Several authors found that different crystal phases gave different gas release rates and apparent diffusion coefficients [1]. The crystal orientation effect is emphasized for the ion bombardment and fission recoil techniques of labelling, i.e., where channelling of the inert gas atoms is possible. Kornelsen and Sinha [29] observed an effect of crystallographic direction of ion bombardment on the inert gas release from single tungsten crystals. Fig. 13 shows variations of Xe release spectra of tungsten crystals for identical 400 eV-Xe bombardment of three different faces ⟨110⟩, ⟨100⟩ and ⟨211⟩. Similarly Matzke [10] obtained different values of diffusion activation energy from release curves of SiO_2 crystals bombarded with 40 keV xenon. At low dose (8×10^{10} ions sm^{-2}) diffusion release along and perpendicular to the *c*-axis dominated with activation energy values of 243 and 255.4 kJ $mole^{-1}$, respec-

tively. A value 301 kJ mole^{-1} was found for Xe-bombarded fused silica. Diffusion in the amorphous phase was markedly slower than the diffusion in the crystalline phase.

8.3. *Morphology changes in bulk ceramics and thin films*

The changes in morphology taking place during aging, drying, calcination and firing of feed or intermediate geleous materials can be successfully investigated by TIGRA. The method was used for quality testing of intermediate geleous products of urania, titania, silica, zirconia, etc. [30–33]. Thin ceramic films can also be investigated. TIGRA is sensitive to the morphology changes caused by deviations of technological conditions; therefore it has been recommended as the control method for quality testing intermediate products of sol–gel processed ceramics both in bulk and thin films. The morphology changes of $TaSi_2$ thin layers (transition from a very disordered state to a crystalline one) were revealed by the measurement of argon release which was included in the structure defects of the thin film prepared by sputtering [34] (see Fig. 14).

TIGRA was used in the characterization of thermal behaviour of titania (rutile) The experimental results obtained by Beckman [17], made it possible to deter-

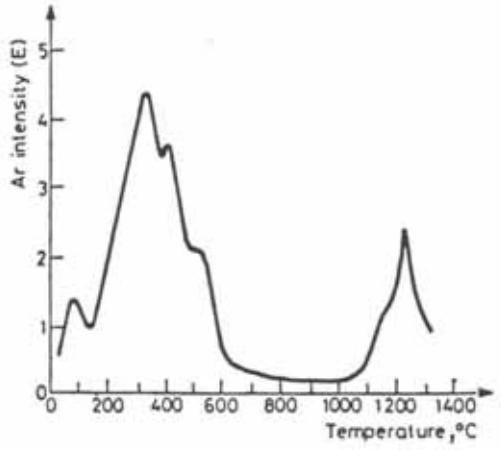

Fig. 14. Temperature dependence of argon release rate from 250 nm thick $TaSi_2$ thin film deposited by sputtering in argon atmosphere (argon atoms were captured during the sputtering process in the thin film defects).

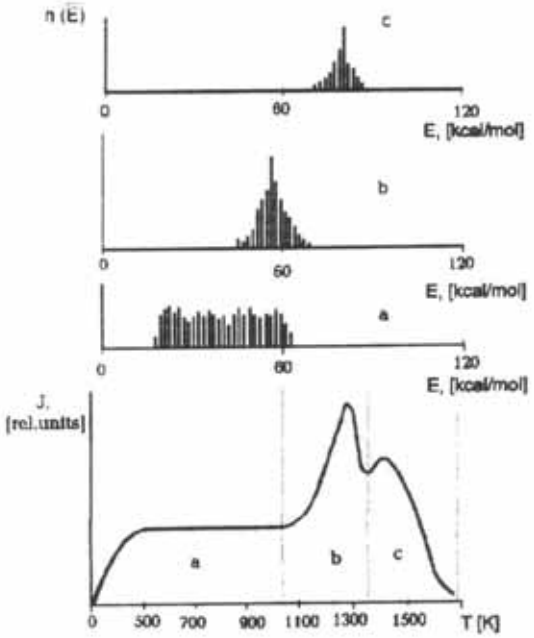

Fig. 15. **Upper part**: The spectra of activation energy values (parts a,b,c) determined from the TIGRA experiments in the diagnostics of rutile sample. **Lower part**: The temperature dependence of the thermostimulated radon release from rutile powder. (Heating in air at a heating rate of 5 K min^{-1}).

mine the activation energies of the inert gas migration controlled by the mobility of the structure defects of different types. The experimental results were treated by means of the DIGS software using the "single-jump diffusion" model. The inert gas (radon) was introduced into the surface near layers of rutile in the low temperature glow discharge according to Jech [9]. The release of radon at the temperature from 300 to 900 K (see Fig. 15–the temperature interval denoted α) corresponds to the continuous activation energy spectrum (spectrum a), where the E_{min}=19 kcal mol^{-1}, E_{max}=63 kcal mol^{-1}. The radon release rate at the temperatures above 1250 K is controlled by the diffusion characterized by a narrow spectrum of the activation energies: E_{min}= 45 kcal mol^{-1}, E_{mean}=57 kcal mol^{-1}, E_{min}=64 kcal mol^{-1} (the energy spectrum b). The activation energy values of this process correlate well that of self-diffusion of Ti cation in the rutile lattice. The maximum of the temperature dependence of radon release rate at the temperature of 1450 K corresponds to the

inert gas release denoted as **stage IIb**, by Matzke [10]. The activation energy values determined from the experimental results of TIGRA are as follows: E_{min}=69 kcal, E_{mean}=3 kcal mol^{-1}, E_{max}= 85 kcal mol^{-1} (see the energy spectrum c). The thermal behaviour of rutile sinters using inert gas release was described by Kelly and Matzke [35]. A good agreement of the results presented in [35] and [17] was found.

9. Conclusion

The thermostimulated inert gas release analysis, TIGRA, can be recommended as a sensitive tool for the diagnostics of materials, making it possible to reveal annealing natural and radiation defects, order–disorder transition and other changes in the solids which may influence the mobility of inert gas atoms in the solids investigated. By this method a supplementary information to that obtained by traditional thermal analysis methods can be obtained. This is especially important in the characterisation of high technology materials, single crystals, thin films, ceramics, etc.

References

[1] V. Balek and J. Tolgyessy, in: Wilson and Wilson (Eds.), Emanation thermal analysis and other radiometric emanation methods, Comprehensive Analytical Chemistry, Part XIIC, Elsevier, Amsterdam (1984) pp. 304 .
[2] V. Balek, Thermochim Acta, 148 (1989) 11.
[3] V. Balek, Thermochim Acta, 192 (1991) 1.
[4] V. Jesenak, S. Varga and J. Tolgyessy, Atompraxis, 14 (1968) 204.
[5] V. Jesenak, J. Tolgyessy and E.H. Kehr, Radiochem. Radional letters, 19 (1994) 223.
[6] G.Dearnaley, J.H.Freeman, R.S.Nelson and J.Stephen, Ion Implantation, North Holland, Amsterdam (1993).
[7] J.A. Davies, F. Brown and M. Mc.Cargo, Can. J. Phys., 41 (1963) 829.
[8] I. Bergstrom, F. Brown, J.A. Davies, J.S. Geiger, R.L. Craham and R. Kelly, J.Nucl.Instr, and Methods, 21 (1963) 249.
[9] C. Jech, Int. J. Appl. Rad. and Isotopes, 8 (1965) 19.
[10] H.J.Matzke, in B. Navinsek (Ed.), Physics of Ionised Gases, Institut Josef Stefan, Lubljana, Yugoslavia, 1970, p. 326.
[11] A.A. Shviryaev, I.N. Beckman and V. Balek, Thermochim Acta, 111 (1987) 215.
[12] R. Kelly and H.J. Matzke, J.Nucl.Mat., 20 (1966) 11.
[13] R. Kelly, C. Jech and H.J. Matzke, Phys. Stat. Sol., 25 (1968) 641.
[14] D.R.Hurst, Report AECL-1550 (1962).
[15] I.N.Beckman, in D.R.Paul, Y.P.Yampol'skii (Eds.), Polymeric gas separation membranes, CRC Press, Boca Raton, FL (1994).
[16] I.N. Beckman and I.P. Romanovskii, Uspekhi Khimii (Rus.), 5 (1988) 944.
[17] I.N. Beckman, in V. Balek and J. Tolgyessy (Eds.), Emanation Thermal Analysis, Suppl, to Russian Translation, Mir, Moscow, Russia (1986) p. 309.
[18] H.J. Matzke, Z. Naturforsch, 22a (1967) 507.
[19] I.N. Beckman, D.G. Bessarabov, R.D. Sanderson, in Proc. Int. Conf, EUROMEMRANE 95, Bath, UK, Vol.2 (1995) p. 182.
[20] A.V. Zheleznov, I.N. Beckman and V. Balek, Thermochim. Acta, 142 (1989) 241.
[21] A.V. Zheleznov, I.N. Beckman and V. Balek, Thermochim. Acta, 143 (1989) 2.
[22] I.N. Beckman, A.A. Shviryaev. V. Balek, in Synthetic polymeric membranes, Proc. 29th Microsymposium Prague, Czech Republic (1996) SL 17.
[23] I.N. Beckman, Thermochim. Acta, 190 (1991) 66.
[24] I.N. Beckman, A.N. Zheleznov and V. Balek, J. Therm. Anal., 37 (1991) 149.
[25] V. Balek, I.N. Beckman and A.V. Zheleznov, J. Therm. Anal., 39 (1993) 1019.
[26] I.N. Beckman, A.A. Shviryaev and V. Balek, Thermochim Acta, 104 (1986) 255.
[27] E.V. Kornelsen and M.K. Sinha, J. Appl. Phys., 39 (1968) 4546.
[28] C. Jech, R. Kelly and J. Phys, Chem. Sol., 30 (1969) 465.
[29] E.V. Kornelsen and M.K. Sinha, Appl. Phys. Letters, 9 (1966) 112.
[30] V. Balek, J. Nucl. Mater., 153 (1988) 41.
[31] V. Balek, J. Therm. Anal., 35 (1989) 404.
[32] V. Balek, Sprechsaal Int. Ceram. Glass Mag., 118 (1985) 606.
[33] V. Balek and I.N. Beckman, Thermochim. Acta, 85 (1985) 15.
[34] R.A. Levy and P.K. Gallagher, J. Electrochem. Soc., 132 (1985) 1986.
[35] R. Kelly and H.J. Matzke, J. Nucl. Mat, 20 (1966) 11.